Conditions for microwave amplification due to spin-torque dynamics in magnetic tunnel junctions

Lin Xue,[1] Chen Wang,[1] Yong-Tao Cui,[1] J. A. Katine,[2] R. A. Buhrman,[1] and D. C. Ralph[1,3,a)]
[1]*Cornell University, Ithaca, New York 14853, USA*
[2]*Hitachi Global Storage Technologies, San Jose, California 95135, USA*
[3]*Kavli Institute at Cornell, Ithaca, New York 14853, USA*

(Received 14 March 2011; accepted 12 June 2011; published online 13 July 2011)

Spin torque from a microwave current flowing through a magnetic tunnel junction (MTJ) can excite resonant magnetic dynamics and hence resistance oscillations. When a DC current is also applied, the MTJ produces an oscillating voltage at the frequency of the input signal. This oscillating voltage increases with DC bias and can in principle become larger than the input signal, yielding amplification. We analyze how to design tunnel junction devices to achieve gains larger than one. © *2011 American Institute of Physics*. [doi:10.1063/1.3606550]

Spin transfer torque allows efficient current-controlled manipulation of the magnetic moment in magnetic devices.[1–3] This mechanism is being applied rapidly for technology: spin-torque-controlled magnetic nonvolatile random access memory is nearing commercialization,[4] and other potentially useful devices have been demonstrated including frequency-tunable microwave sources,[5–7] frequency modulators,[8,9] and microwave detectors.[10,11] Here, we analyze another potential application of spin-torque devices, as microwave-frequency amplifiers.

The idea of making a microwave amplifier using spin torque was first proposed by Slonczewski,[12] and other amplification schemes have been proposed using negative differential resistance[13] or magnetic vortex oscillations.[14,15] The mechanism of gain we will consider is illustrated for a simple 2-terminal magnetic tunnel junction (MTJ) in Fig. 1(a). An input microwave signal, V_{in}, generates resonant magnetic precession via a spin-transfer torque exerted on one electrode of the MTJ and thereby produces resistance oscillations. If a DC current is also applied, the oscillating resistance produces an oscillating voltage by Ohm's law that can be transmitted out of the MTJ as a reflected signal V_{ref}. If the applied DC current is sufficiently large, then the reflected signal can be larger than the input signal, yielding amplification. We will analyze the simplest case in which the MTJ magnetic layers are in-plane in equilibrium, and the microwave drive excites small-angle, approximately spatially uniform magnetic precession.

The high-frequency signal generated by a MTJ in response to a microwave-frequency input can be calculated using microwave circuit equations together with methods to analyze the magnetic dynamics similar to those employed for spin-torque ferromagnetic resonance[10,16,17] and thermally excited ferromagnetic resonance.[18] Assuming that the waveguide contacting the sample has a 50 Ω impedance, the reflected signal arising from an input signal $V_{in}(\omega)$ together with an oscillating resistance is

$$V_{ref}(\omega) = \frac{R_0 - (50\,\Omega)}{R_0 + (50\,\Omega)} V_{in}(\omega) + \frac{(50\,\Omega)}{R_0 + (50\,\Omega)} I_{DC} \Delta R(\omega), \quad (1)$$

where R_0 is the differential resistance of the MTJ and $\Delta R(\omega)$ is the oscillating part of the DC resistance. The first term is the reflection that results from impedance mismatch between the 50 Ω waveguide and the MTJ, and the second term is the signal generated by the oscillating resistance. We assume small angle precession, so that $\Delta R(\omega) = \partial R/\partial\theta|_I \delta\theta(\omega)$, where θ is the angle between the magnetizations of the two electrodes of the MTJ. To calculate the precession angle $\delta\theta(\omega)$, we approximate the magnetization of the free layer in the MTJ (the one that precesses) as a spatially uniform macrospin with direction $\hat{m}$, we assume that the other magnetic electrode remains fixed, and we use the Landau-Lifshitz-Gilbert-Slonczewski equation of motion:[1,3]

$$\frac{d\hat{m}}{dt} = -\gamma \hat{m} \times \vec{H}_{\text{eff}} + \alpha \hat{m} \times \frac{d\hat{m}}{dt} + \gamma \frac{\tau_{||}(V,\theta)}{M_s Vol} \hat{m} \times \frac{\hat{m} \times \hat{M}}{|\hat{m} \times \hat{M}|} + \gamma \frac{\tau_{\perp}(V,\theta)}{M_s Vol} \frac{\hat{m} \times \hat{M}}{|\hat{m} \times \hat{M}|}. \quad (2)$$

Here, $\vec{H}_{\text{eff}}$ is the effective field acting on the free layer including the applied, demagnetization, and exchange fields; α is the Gilbert damping parameter; $M_S Vol$ is the total moment of the free layer; $\tau_{||}(V,\theta)$ and $\tau_{\perp}(V,\theta)$ are the "in-plane" and "perpendicular" components of the spin torque;[17] $V = V_{DC} + \delta V(\omega)$ is the voltage across the MTJ; and γ is the absolute value of the gyromagnetic ratio. The final ingredient for a closed set of equations is to relate $\delta V(\omega)$, the oscillating part of the voltage across the MTJ, to the input and reflected voltages:

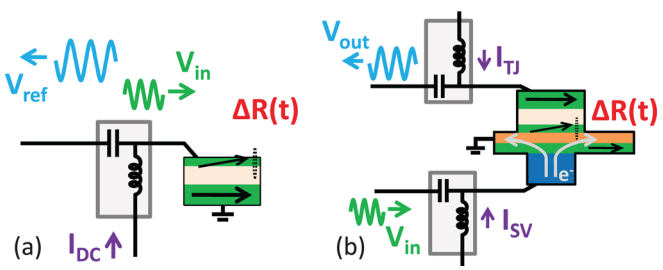

FIG. 1. (Color online) (a) Illustration of the mechanism of amplification for a standard 2-terminal magnetic tunnel junction. (b) Proposed design for a 3-terminal device.

a)Author to whom correspondence should be addressed. Electronic mail: ralph@ccmr.cornell.edu.

$$\delta V(\omega) = V_{in}(\omega) + V_{ref}(\omega) = \frac{2R_0}{R_0 + (50\,\Omega)} V_{in} + \frac{(50\,\Omega) I_{DC} \Delta R(\omega)}{R_0 + (50\,\Omega)}. \quad (3)$$

This expression takes into account a feedback mechanism[19] that the oscillating resistance will alter the voltage across the MTJ and will thus affect the spin torque that drives the oscillation.

By solving Eqs. (1)–(3) for a circular 2-terminal MTJ for which the magnetizations of both electrodes lie in the sample plane in equilibrium, we calculate a (complex-valued) voltage gain:

$$S_{11} \equiv \frac{V_{ref}}{V_{in}} = \frac{R_0 - (50\,\Omega)}{R_0 + (50\,\Omega)} + \frac{(50\,\Omega)}{R_0 + (50\,\Omega)} I_{DC} \chi(\omega), \quad (4)$$

where

$$\chi(\omega) \equiv \Delta R(\omega)/V_{in} = -\left.\frac{\partial R}{\partial \theta}\right|_I \frac{R_0}{R_0 + (50\,\Omega)} \frac{\gamma}{M_S Vol} \times \frac{1}{\omega - \omega_m - i\sigma} \left[i \left.\frac{\partial \tau_{||}}{\partial V}\right|_\theta + \frac{\gamma N_x M_{\rm eff}}{\omega_m} \left.\frac{\partial \tau_\perp}{\partial V}\right|_\theta \right], \quad (5)$$

$$\omega_m \approx \gamma M_{\rm eff} \sqrt{N_x \left[N_y - \frac{1}{M_{\rm eff} M_S Vol} \left(\left.\frac{\partial \tau_\perp}{\partial \theta}\right|_V + \frac{(50\Omega)}{R_0 + (50\Omega)} I_{DC} \left.\frac{\partial R}{\partial \theta}\right|_I \left.\frac{\partial \tau_\perp}{\partial V}\right|_\theta \right) \right]}, \quad (6)$$

$$\sigma \approx \frac{\alpha \gamma M_{\rm eff} (N_x + N_y)}{2} - \frac{\gamma}{M_S Vol} \left(\left.\frac{\partial \tau_{||}}{\partial \theta}\right|_V + \frac{1}{2} \frac{(50\,\Omega)}{R_0 + (50\,\Omega)} I_{DC} \left.\frac{\partial R}{\partial \theta}\right|_I \left.\frac{\partial \tau_{||}}{\partial V}\right|_\theta \right). \quad (7)$$

Here, $N_x = 4\pi + H/M_{\rm eff}$, $N_y \approx H/M_{\rm eff}$, $4\pi M_{\rm eff}$ is the strength of the easy-plane anisotropy field, and H is component of applied magnetic field along the precession axis. The real and imaginary parts of S_{11} correspond to the in-phase and out-of-phase response. This calculation predicts resonance peaks at the ferromagnetic resonance frequency, with line shapes as a function of frequency as plotted in Fig. 2. We have verified that the calculated signals are in good agreement with network-analyzer measurements on (unoptimized) CoFeB/MgO/CoFeB MTJs (Figs. 2(c) and 2(d)), although for these samples the gains are much less than 1.

We can estimate what is the maximum possible voltage gain from a simple 2-terminal MTJ by evaluating Eq. (4) using the following optimistic but reasonable parameters: resistance for parallel electrode magnetizations $R_P = 50\ \Omega$; tunneling magnetoresistance, TMR = 150%; $M_S Vol = 5.8 \times 10^{-15}$ emu; $\alpha = 0.01$; $H = 100$ Oe; $4\pi M_{\rm eff} = 1.1$ kOe (assuming a reduction by about factor of 10 compared to a typical metal ferromagnet due to the introduction of perpendicular magnetic anisotropy[20]); $\tau_\perp(V,\theta) \approx 3.8\ {\rm V}^2 \sin\theta (\hbar/2e)\,{\rm k}\Omega^{-1}{\rm V}^{-1}$, and $\tau_{||}(V,\theta) \approx 6.9\ V \sin\theta (\hbar/2e){\rm k}\Omega^{-1}$. These spin-torque values are determined by scaling the results in Fig. 3(b) of Ref. 21 inversely by the ratio of the samples' zero-bias parallel resistances and assuming for simplicity that $\tau_\perp \propto V^2$ and $\tau_{||} \propto V$. In Figures 3(a), 3(c) and 3(d), we plot the magnitude of the maximum change in S_{11} near resonance. We find that voltage gains greater than one are possible, but they require fine-tuning the offset angle and $I_{\rm DC}$ very precisely to bias the sample near the critical current where the bias-dependent linewidth σ goes to zero, the threshold for exciting DC-driven auto-oscillations. Somewhat better amplification might be achievable using devices biased to generate nonlinear, large-angle precessional dynamics[22] not described within our small-angle approximation, but nevertheless we conclude that this need for fine-tuning near a point of singular dynamics (i.e., adjusting for time-dependent sample variations and thermal fluctuations) likely prohibits the use of simple 2-terminal MTJs for microwave amplifier applications.

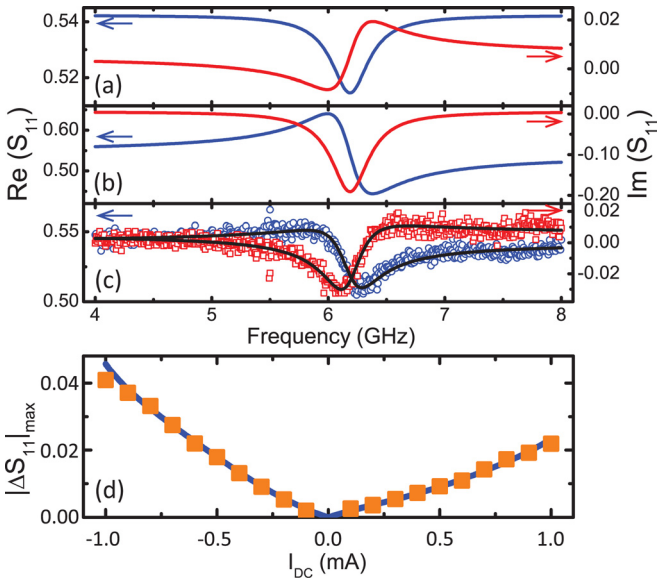

FIG. 2. (Color online) The high-frequency response of 2-terminal MTJs. (a),(b) Calculated frequency dependence for the real (blue lines, left axes) and imaginary (red lines, right axes) parts of S_{11} for (a) a purely in-plane spin torque and (b) a purely out-of-plane spin torque. When both torque components are present, S_{11} is a weighted sum of the two contributions. (c) Points: Real and imaginary parts of the measured S_{11} signal for a CoFeB/MgO/CoFeB MTJ with $R_P = 122\ \Omega$, TMR = 78% and $RA = 1.0\ \Omega\ \mu{\rm m}^2$ for $I_{DC} = -1.0$ mA and $H = 300$ Oe applied 145° from the fixed-layer's exchange bias direction. The lines are fits to Eq. (4) with the fit values $\partial\tau_{||}/\partial V|_\theta = 2.8 \pm 0.5 (\hbar/2e){\rm k}\Omega^{-1}$ and $\partial\tau_\perp/\partial V|_\theta = -0.5 \pm 0.1 (\hbar/2e){\rm k}\Omega^{-1}$. (d) Points: measured gain for the same unoptimized MTJ and field bias. Line: prediction of Eq. (4) for $\partial\tau_{||}/\partial V|_\theta = 1.8(\hbar/2e){\rm k}\Omega^{-1} - 930 I (\hbar/2e)\,{\rm kV}^{-1}$ and $\partial\tau_\perp/\partial V|_\theta = -0.06\ (\hbar/2e){\rm k}\Omega^{-1} + 520 I\ (\hbar/2e){\rm kV}^{-1}$.

Larger, controllable gains should be achievable in 3-terminal devices. This was the approach originally proposed by Slonczewski.[12] We consider a geometry similar to the devices recently studied by Sun *et al.*[23] (Fig. 1(b)), consisting of a lower CoFe/Cu/CoFeB all-metal, low-resistance spin valve in which the CoFeB free layer (assumed circular) can be manipulated by spin torque via non-local spin injection, together with a MgO/CoFeB tunnel junction cap by which the moving free layer can generate large resistance oscillations. This geometry can facilitate the application of large microwave currents through port 1 to the metal spin valve to generate large free-layer oscillations, with the possibility to use a DC current I_{SV} through the spin valve to control the bias-dependent linewidth to be stably close to zero. The large-TMR MTJ with a separate DC bias I_{TJ} generates the output signal through port 2. We can use an analysis similar

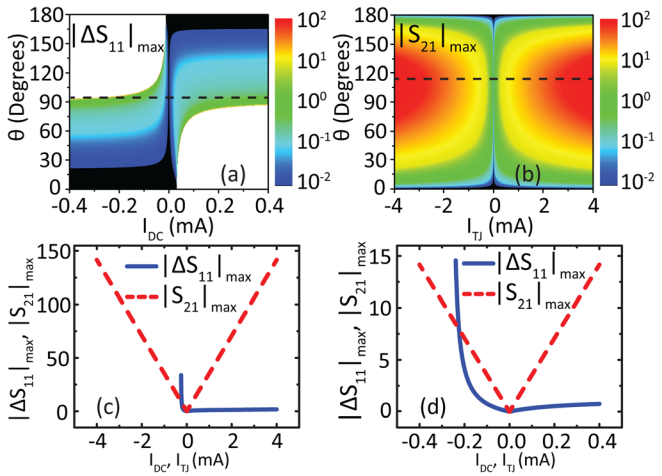

FIG. 3. (Color) (a) Log-scale color plot of the calculated maximum value of $|\Delta S_{11}|$ for an optimized 2-terminal MTJ, as a function of I_{DC} and the offset angle θ between the magnetization directions of the two electrodes. The white regions at the upper left and lower right represent parts of the phase diagram where the DC current generates auto-oscillations with no applied oscillatory current. (b) Log-scale color plot of the calculated maximum value of $|S_{21}|$ for an optimized 3-terminal MTJ, as a function of the DC current through the MTJ and the offset angle θ between the magnetizations of the MTJ electrodes. (c) Comparison of the voltage gain factors for optimized 2-terminal and 3-terminal MTJs, for the values of θ shown by dotted lines in (a) and (b). The current on the horizontal axis corresponds to the DC current applied to the MTJ (not the spin valve in the 3-terminal device). (d) Zoom-in of the data in (c), showing the detailed dependence near zero current.

to that employed above to estimate the voltage gain (S_{21}). Assuming that the differential resistance for the MTJ is R_0 and for the spin valve is R_{SV}, the DC resistance of the MTJ is R_{TJ} and the equilibrium orientations of all three magnetic layers are in the sample plane,

$$S_{21} = \frac{V_{out}}{V_{in}} = -\frac{I_{TJ}}{R_0 + (50\,\Omega)}\left(\frac{2(50\,\Omega)}{R_{SV} + (50\,\Omega)}\right)\frac{\partial R_{TJ}}{\partial \theta}\frac{\gamma}{2M_S Vol} \times \left(\frac{1}{\omega - \omega_m - i\sigma}\right) i\frac{\partial \tau_{||}}{\partial I_{SV}}\bigg|_{\theta}. \quad (8)$$

We have not included a perpendicular component of torque because this component should be absent for all-metal spin valves.[16] For estimation purposes, we use the optimistic parameters: R_{TJ}= 50 Ω in the parallel configuration, TMR = 150%, R_{SV} = 3 Ω, $M_S Vol = 5.8 \times 10^{-15}$emu, $\partial\tau_{||}/\partial I_{SV}|_{\theta} = 0.4 \sin\theta_{SV}(\hbar/2e)$, [24] and $\sigma = 3 \times 10^7$ rad/s (this is a factor of 100 reduction compared to a typical transition metal ferromagnet; we assume a factor of 10 reduction by using perpendicular anisotropy to reduce $4\pi M_{\text{eff}}$ (Ref. 20) and another factor of 10 by using I_{SV} to reduce the bias-dependent linewidth, and we assume I_{SV} is adjusted as a function of I_{TJ} to keep σ constant at this reduced value). Figures 3(b)–3(d) show the calculated value of $|S_{21}|$ near resonance as a function of I_{TJ} and θ . This calculation indicates that a voltage gain larger than 100 is achievable using physically reasonable materials parameters. The associated power gain-bandwidth product is $|S_{21}(\omega_m)|^2\sigma/\pi \sim 200$ GHz and scales $\propto 1/\sigma$. Even larger gains may be possible using other sample geometries (e.g., employing a reference layer polarized out of plane, while the free layer remains polarized in plane) or by applying out-of-plane magnetic field to achieve a large-angle, nonlinear magnetic response.[22]

Our analysis also does not yet include consideration of noise.[25] The output noise of the amplifier associated with thermal fluctuations of the free layer will increase as the volume of the free layer is decreased so as to maximize the gain. This will likely constrain the values of $M_S Vol$ and H that can be employed when optimizing device properties.

In summary, we have analyzed the conditions under which MTJ-based devices might be used to generate resonant microwave amplification. Gain greater than 1 is possible in principle even in simple 2-terminal tunnel junctions, but is unlikely to be controllable because this requires biasing the sample very close to a point of singular dynamics where the bias-dependent linewidth goes to zero. However, 3-terminal tunnel-junction devices should be able to achieve controllable microwave voltage gains of at least 100.

Cornell acknowledges support from ARO, ONR, NSF (DMR-1010768), and the NSF/NSEC program through the Cornell Center for Nanoscale Systems. We also acknowledge NSF support through use of the Cornell Nanofabrication Facility/NNIN and the Cornell Center for Materials Research facilities.

[1] J. C. Slonczewski, J. Magn. Magn. Mater. **159**, L1 (1996).
[2] L. Berger, Phys. Rev. B **54**, 9353 (1996).
[3] D. C. Ralph and M. D. Stiles, J. Magn. Magn. Mater. **320**, 1190 (2008).
[4] J. M. Slaughter, Annu. Rev. Mater. Res. **39**, 277 (2009).
[5] S. I. Kiselev *et al.*, Nature **425**, 380 (2003).
[6] W. H. Rippard *et al.*, Phys. Rev. Lett. **92**, 027201 (2004).
[7] D. Houssameddine *et al.*, Phys. Rev. Lett. **102**, 257202 (2009).
[8] M. R. Pufall *et al.*, Appl. Phys. Lett. **86**, 082506 (2005).
[9] B. Georges *et al.*, Appl. Phys. Express **2**, 123003 (2009).
[10] A. A. Tulapurkar *et al.*, Nature **438**, 339 (2005).
[11] S. Ishibashi *et al.*, Appl. Phys. Express **3**, 073001 (2010).
[12] J. C. Slonczewski, U.S. patent 5,695,864 (9 December 1997).
[13] Y. Suzuki and H. Kubota, J. Phys. Soc. Jpn. **77**, 031002 (2008).
[14] S. Kasai *et al.*, Appl. Phys. Express **1**, 091302 (2008).
[15] T. Nozaki *et al.*, Appl. Phys. Lett. **95**, 022513 (2009).
[16] J. C. Sankey *et al.*, Phys. Rev. Lett. **96**, 227601 (2006).
[17] C. Wang *et al.*, Phys. Rev. B **79**, 224416 (2009).
[18] S. Petit *et al.*, Phys. Rev. Lett. **98**, 077203 (2007).
[19] S. Garzon *et al.*, J. Magn. Magn. Mater. **321**, 3225 (2009).
[20] L. Liu *et al.*, Appl. Phys. Lett. **94**, 122508 (2009).
[21] C. Wang *et al.*, Nat. Phys. **7**, 496 (2011).
[22] X. Cheng *et al.*, Phys. Rev. Lett. **105**, 047202 (2010).
[23] J. Z. Sun *et al.*, Appl. Phys. Lett. **95**, 083506 (2009).
[24] J. Xiao, A. Zangwill, and M. D. Stiles, Phys. Rev. B **72**, 014446 (2005).
[25] A. Slavin and V. Tiberkevich, IEEE Trans. Magn. **45**, 1875 (2009).